THERMAL DIFFUSION OF ZINC FROM ZINC-CONTAINING BOROSILICATE GLASS INTO CADMIUM CHALCOGENIDE NANOCRYSTALS

Yu.M. Azhniuk[1)], V. Stoyka[2)], V.V. Lopushansky[1)], I. Petryshynets[2)], F. Kováč[2)], A.V. Gomonnai[1)], D.R.T. Zahn[3)]*

[1)] Institute of Electron Physics, Ukr. Nat.Acad. Sci., Universytetska Str. 21, Uzhhorod, 88017, Ukraine

[2)] Institute of Materials Science, Slovak Academy of Sciences, Watsonova 47, Košice 04001, Slovakia

[3)] Semiconductor Physics, Chemnitz University of Technology, D-09107, Chemnitz, Germany

Received 24.11.2011
Accepted 06.03.2012

**Corresponding author: e-mail: yu.azhniuk@gmail.com, telephone: +380 312 643822, fax: +380 312 643650, Institute of Electron Physics, Ukr. Nat.Acad. Sci., Universytetska Str. 21, Uzhhorod, 88017, Ukraine*

Abstract

Studies of Raman scattering spectra and scanning electron microscopy imaging combined with energy-dispersive X-ray spectroscopy data of II-VI semiconductor nanocrystals formed in zinc-containing borosilicate glass matrix are carried out. It is shown that diffusion of zinc from the matrix at 625 to 700 °C results in the formation of mixed $Cd_{1-y}Zn_yS_{1-x}Se_x$ nanocrystals with Zn content up to 30 %, as determined from the LO phonon frequencies. An increase of the Zn content in the nanocrystals with the thermal treatment temperature and duration is observed. A uniform distribution of zinc over the nanocrystal volume is assumed based on the diffusion coefficient data.

Keywords: interface diffusion, annealing, scanning electron microscopy (SEM), energy dispersive X-ray spectroscopy (EDXS), compound semiconductors, nanocrystalline materials, Raman spectroscopy.

1 Introduction

Diffusion-limited growth from a supersaturated solution in a silicate glass is a well-known technique to obtain dilute semiconductor nanocrystals embedded in a dielectric matrix [1–6]. It is well elaborated for fabrication of binary and ternary II-VI cadmium chalcogenide nanocrystals in borosilicate glass traditionally used as optical cutoff filters in the spectral range from yellow to near infrared and considered as promising materials for non-linear optical applications [4]. Diffusion-limited growth takes place at thermal treatment in the range from 500 to 700°C. The average size of nanocrystals increases with the thermal treatment temperature and duration. Several studies were devoted to the dependence of ternary (mostly $CdS_{1-x}Se_x$) nanocrystal composition on the thermal treatment parameters [5, 6]. Besides, experimental evidence for zinc incorporation from zinc-containing matrices into CdS [7–10] and $CdS_{1-x}Se_x$ [11, 12] nanocrystals was reported.

Here we report on scanning electron microscopy and Raman scattering studies of thermal diffusion of zinc into II-VI nanocrystals in zinc-containing borosilicate glass and formation of ternary ($Cd_{1-x}Zn_xS$) and quaternary ($Cd_{1-y}Zn_yS_{1-x}Se_x$) nanocrystals.

2 Materials and experimental methods

II-VI nanocrystals were obtained in borosilicate glass by diffusion-limited growth from commercially available LZOS or Schott cutoff filters which were heated to 1000°C for 2 h. This resulted in the glass melting and decolouring, the existing nanocrystals were thus dissolved in the borosilicate glass, providing a random distribution of cadmium and chalcogen atoms over the borosilicate glass structural network. After rapid quenching the obtained colourless transparent glass samples were cut into pieces and subjected to thermal treatment at controlled temperatures within the range from 600 to 700°C. Consequently, batches of samples prepared from the same initial mixture at different thermal treatment temperatures and durations were obtained.

Scanning electron microscopy (SEM) studies combined with energy dispersive X-ray spectroscopy (EDX) were performed using a SEM JEOL 7000F microscope.

Raman spectra were measured using a Dilor XY 800 spectrometer with a CCD camera, the excitation was provided by an Ar^+ laser (λ_{exc} = 457.9, 476.5, 488 and 514.5 nm). The instrumental width was better than 2.5 cm^{-1}. No noticeable differences were revealed between the spectra measured in macro-and micro-Raman scattering configurations. In many cases the Raman spectra were observed with a background of a broad phtoluminescence band which was subsequently subtracted for the analysis of the Raman spectra. Optical absorption spectra were measured with a LOMO MDR-23 spectrometer. All measurements were carried out at 293 K.

3 Results and discussion

As can be seen from **Fig. 1**, SEM studies combined with EDX elemental analysis enabled us to choose samples where the glass matrix contained a considerable amount of zinc. Note that no traces of cadmium, sulphur, or selenium could be noticed from the EDX data since the cadmium chalcogenide fraction in the glass matrix does not exceed 1 % which is below the measurement sensitivity level.

Optical absorption spectra of samples obtained from the same batch of the zinc-containing glass doped with Cd, S, and Se at various thermal treatment durations and temperatures are shown in Fig. 2. A sharp edge observed in the absorption spectrum is evidence for the formation of II-VI semiconductor nanocrystals in the glass matrix. If the average nanocrystal radius is below the Bohr exciton radius for the given compound one can observe characteristic confinement-related maxima at the absorption edge at the energies given by [13]

$$E_{(n_e,l_e),(n_h,l_h)} = E_b + \frac{\hbar^2}{2r^2}\left[\frac{\varphi^2_{n_e,l_e}}{m_e^*} + \frac{\varphi^2_{n_h,l_h}}{m_h^*}\right] \tag{1.}$$

where E_b is the energy gap for the bulk material, r is the nanocrystal radius, $\varphi_{n,l}$ are spherical Bessel function roots for the corresponding quantum numbers, m_e^* and m_h^* are effective masses of electrons and holes, respectively. One can estimate the average nanocrystal radius from the most pronounced first confinement-related maximum energy position E_1 ($\varphi_{n,l}$=1). Besides, since the II-VI nanocrystals undergo a considerable (near 0.5 GPa) pressure from the glass matrix (due to the difference in thermal expansion coefficients of the semiconductor nanocrystals and the matrix), one should take into account the pressure-related energy gap variation ΔE_g^p:

$$E_1 = E_b + \Delta E_g^p + \frac{\hbar^2}{2r^2}\left[\frac{1}{m_e^*} + \frac{1}{m_h^*}\right]. \tag{2.}$$

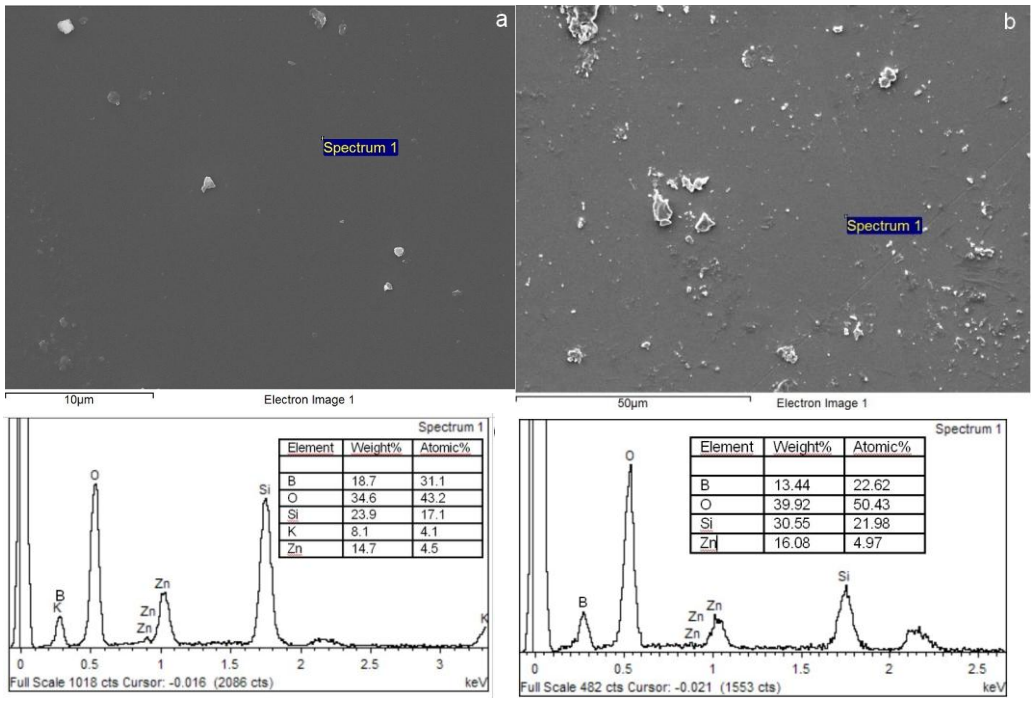

Fig.1 SEM images of two zinc-containing borosilicate glass samples as well as their EDX spectra with the corresponding elemental composition determined from the EDX data.

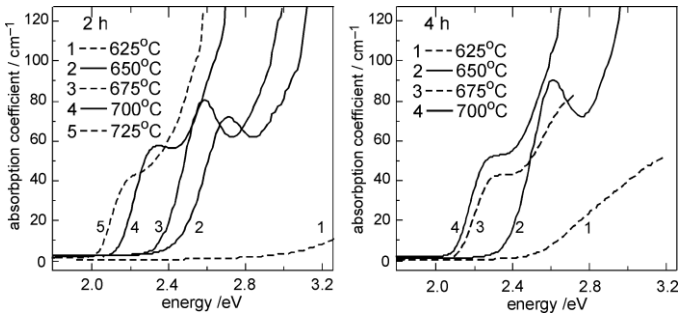

Fig.2 Optical absorption spectra of zinc-containing borosilicate glass doped with Cd, S, and Se, after heat treatment.

As can be seen from **Fig. 2**, a considerable red shift of the optical absorption edge and the confinement-related maxima with the thermal treatment duration τ and temperature T_a is the evidence for the increase in average nanocrystal size.

The most efficient and reliable technique to determine the composition of mixed II-VI semiconductor nanocrystals grown in a glass matrix is Raman spectroscopy which is especially well elaborated for $CdS_{1-x}Se_x$ nanocrystals [14–17]. The $CdS_{1-x}Se_x$ mixed crystal system exhibits two-mode compositional behaviour of the phonon spectrum containing CdSe-like TO_1 and LO_1 as well as CdS-like TO_2 and LO_2 phonon modes [14–17]. Meanwhile, $Cd_{1-y}Zn_yS$ [7–10] and $Cd_{1-y}Zn_ySe$ [18–20] ternary systems reveal a one-mode behaviour with only one pair of TO and LO phonons for each intermediate composition, both frequencies gradually increasing with *y*.

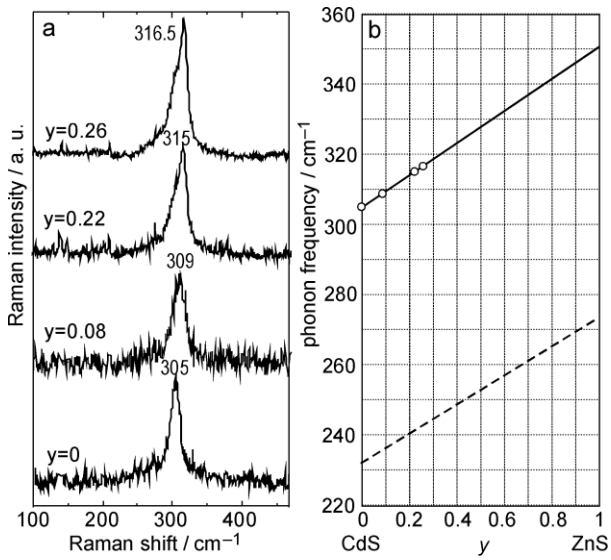

Fig.3 Raman spectra of $Cd_{1-y}Zn_yS$ nanocrystals formed in zinc-containing borosilicate glass doped with Cd and S, under thermal treatment (a) and compositional dependence of LO (solid line) and TO (dashed line) phonon frequencies in $Cd_{1-y}Zn_yS$ (b). The spectra were measured using excitation with λ_{exc} = 457.9 nm.

The fraction of the semiconductor phase in II-VI nanocrystal-doped borosilicate glass is usually very small (below 1 %), hence resonance Raman scattering conditions are important in order to obtain a reliably detectable Raman signal. Therefore, only LO phonon maxima are observed in their Raman spectra since the resonance Raman enhancement is much more pronounced for LO phonons [17]. In the two-mode systems, like $CdS_{1-x}Se_x$, the nanocrystal composition can be determined from the LO phonon peak frequency in the Raman spectra, or, more exactly, from the difference of frequencies of the two LO phonon peaks [14]. In this case the specific effects of phonon confinement [16, 17], surface phonon scattering [15, 16], and glass matrix pressure [21] are better taken into account. With regard to one-mode systems, the nanocrystal composition can be estimated from the frequency of the sole LO phonon in the Raman spectrum. **Fig. 3** a illustrates the experimental first-order Raman spectra of Cd- and S-doped zinc-containing borosilicate glass subjected to intense thermal treatment. The least intense thermal treatment results in the appearance of a Raman peak at 305 cm^{-1} which corresponds to the LO phonon of CdS nanocrystals. The increase of the thermal treatment duration and temperature results in an increase of the LO phonon peak frequency. This can be explained by annealing-induced partial substitution of one of the nanocrystal lattice components by lighter atoms. This cannot be attributed to partial replacement of sulphur in the nanocrystals by oxygen from the glass matrix. Such anion substitution should also have been observed for nanocrystals grown in zinc-free borosilicate matrix while neither our earlier experiments for such systems [6, 22], nor studies performed by other groups [5, 23] have revealed any evidence for annealing-induced increase of LO phonon frequency for glass-embedded II-VI nanocrystals which could be related to substitution of sulphur by oxygen from the glass matrix. Hence, we conclude that the thermal treatment results in a partial substitution of Cd in the nanocrystals by Zn from the matrix and formation of $Cd_{1-y}Zn_yS$ nanocrystals. Knowing the compositional dependence of the LO phonon

frequency in $Cd_{1-y}Zn_yS$ (Fig. 3, b) based on the known Raman data for CdS [24] and ZnS [25] as well as for the mixed crystals [7], one can evaluate the nanocrystal composition. The values corresponding to the experimental data are shown by circles in Fig. 3, b and given explicitly in the spectra of Fig. 3a. It should be noted that in our earlier paper [10] the concentration of zinc in $Cd_{1-y}Zn_yS$ nanocrystals was noticeably underestimated due to a computational error.

A similar behaviour of Raman spectra is observed for zinc-containing borosilicate glass doped with Cd, S, and Se where two LO phonon peaks are observed in the first-order Raman scattering spectra. It can be seen from **Fig. 4a** that for the least intensely annealed sample (625 °C, 2 h), CdSe-like LO_1 and CdS-like LO_2 phonon peaks are observed at 194 and 287.5 cm^{-1}. As follows from the comparison with the known data for $CdS_{1-x}Se_x$ nanocrystals grown in a glass matrix [14, 26], the difference of these frequencies, as the most reliable measure of the chemical composition of glass-embedded ternary nanocrystals with a two-mode behaviour [14, 16, 26], corresponds to a selenium content of x=0.38±0.03. The corresponding composisional dependence of the LO_1 and LO_2 phonon frequencies in $CdS_{1-x}Se_x$ nanocrystals is shown by solid lines in **Fig. 4 b**, and the open circles (denoting the experimentally observed LO_1 and LO_2 phonon frequencies for the least intensely annealed sample) show a good agreement with it.

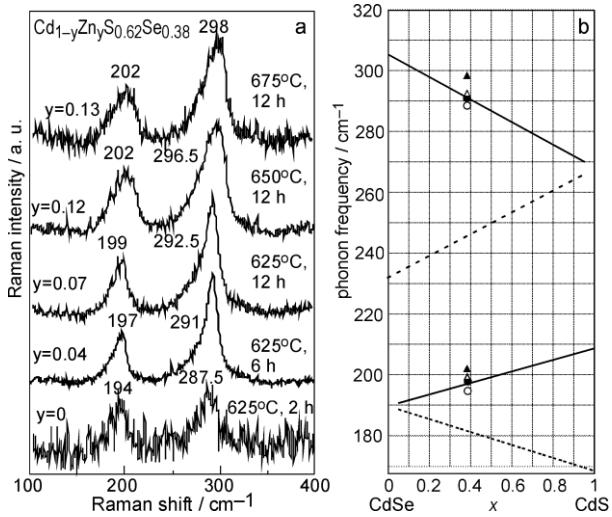

Fig.4 Raman spectra of $Cd_{1-y}Zn_yS_{0.62}Se_{0.38}$ nanocrystals formed in borosilicate glass under thermal treatment (a) and compositional dependence of LO (solid lines) and TO (dashed lines) phonon frequencies in $CdS_{1-x}Se_x$ and the data obtained for the $Cd_{1-y}Zn_yS_{0.62}Se_{0.38}$ nanocrystals (b). The spectra were measured using excitation with λ_{exc} = 488 nm.

With increasing thermal treatment duration τ or temperature T_a, both peaks shift towards higher frequencies, indicating partial substitution of atoms in $CdS_{1-x}Se_x$ nanocrystals by lighter species which, in view of the above discussed reasons, is evidently zinc. Thus, due to the diffusion of zinc from the matrix, quaternary $Cd_{1-y}Zn_yS_{1-x}Se_x$ nanocrystals are formed. Zn content in the nanocrystals can be evaluated from the LO phonon frequencies in the Raman spectra. The phonon frequencies in the spectra increase with τ and T_a, being evidence for the increase of zinc concentration y in the nanocrystals. Since the difference between the LO_2 and LO_1 phonon

frequencies remains practically unchanged, one can assume that the S/Se concentration ratio in the nanocrystals remains constant with τ and T_a. This is apparent from the experimental points in Fig. 4,b while moving from open circles to dark circles and further to open and dark triangles.

Based on the two-mode behaviour of $CdS_{1-x}Se_x$ and $ZnS_{1-x}Se_x$ as well as on the one-mode behaviour of $Cd_{1-y}Zn_yS$ and $Cd_{1-y}Zn_ySe$ systems, one can reasonably assume that the quaternary $Cd_{1-y}Zn_yS_{1-x}Se_x$ system possesses two-mode compositional behaviour with respect to x with selenide-like (LO_1) and sulphide-like (LO_2) phonons, each of them exhibiting one-mode-like frequency shift with y. For one-mode $Cd_{1-y}Zn_yS$ and $Cd_{1-y}Zn_ySe$ ternary systems the compositional shift of the LO phonon frequencies is monotonous and the zinc-induced increment is given by

$$\Delta\nu = 91.4y – 44.2y^2 \ (\text{cm}^{-1}) \ \text{(for } Cd_{1-y}Zn_yS \text{ [9])}, \quad (3.)$$

$$\Delta\nu = 51y – 9y^2 \ (\text{cm}^{-1}) \ \text{(for } Cd_{1-y}Zn_ySe \text{ [18])}. \quad (4.)$$

By weighing Eqs. (3) and (4) by compositional factors (1–x) and x, respectively, the dependences of the selenide-like LO_1 and sulphide-like LO_2 phonon frequencies on the Zn content y for $Cd_{1-y}Zn_yS_{1-x}Se_x$ nanocrystals were obtained [12]. The corresponding values for the samples under investigation are shown in Fig. 4.

However, a parallel upward shift of both LO_1 and LO_2 phonon peaks with heat treatment, consistent with the Cd→Zn substitution in the nanocrystals, is observed only for the samples with comparable content of S and Se (in our case, x=0.38). For the samples with strong predominance of sulphur over selenium or vice versa a clear shift with Zn content increase is observed only for the LO phonon which corresponds to the predominant chalcogen (CdS-like or CdSe-like, respectively). Meanwhile, the "minority" LO phonon maximum (CdSe-like for S-rich and CdS-like for Se-rich $Cd_{1-y}Zn_yS_{1-x}Se_x$ nanocrystals) exhibits a much smaller shift with heat treatment or sometimes even does not shift in frequency at all. Such situation is illustrated by **Fig. 5** where the Raman spectra of a series of samples prepared from the same Cd-, Se-, and S-doped borosilicate glass (with Se content strongly prevailing over S) at different thermal treatment parameters τ and T_a are shown. It is obvious that the frequency of LO_1 phonon corresponding to the predominant Se chalcogen, shifts with annealing from 203 to 220 cm^{-1} while the overall variation of the frequency of LO_2 phonon corresponding to the minority chalcogen (sulphur) varies only within 2–3 cm^{-1}.

A reasonable explanation of such behaviour can be proposed in view of our recent results showing that the composition of $CdS_{1-x}Se_x$ nanocrystals prepared from the same initial mixture depends on the thermal treatment parameters (τ and T_a) and on the ratio of S and Se content in the initial mixture [6]. Namely, with increasing τ and T_a the content of the predominant chalcogen in the nanocrystals increases while the minority chalcogen is pushed out into the matrix. Hence, the increase of the predominant chalcogen (in this case – Se) concentration in the nanocrystals with τ and T_a results in the LO_1 and LO_2 phonon band convergence, as follows from the two-mode behaviour, while a simultaneous effect of increasing zinc diffusion with τ and T_a leads to the upward shift of both LO phonon peaks. This finally results in the observed considerable shift of the selenide-like LO_1 phonon band and the tiny variation of the LO_2 phonon frequency. Taking into account the two effects enabled us to estimate sulphur and selenium content for the nanocrystals of each sample from the LO_2 and LO_1 phonon frequency difference while zinc content y was evaluated from Eqs. (3) and (4) weighed by the corresponding (1–x) and x factors. The points in Fig. 5, b clearly show the increase of the Zn-induced increment of the LO_1 and LO_2 phonon frequencies over the corresponding values for $CdS_{1-x}Se_x$ nanocrystals with τ and T_a (from open circles to dark circles, triangles and squares).

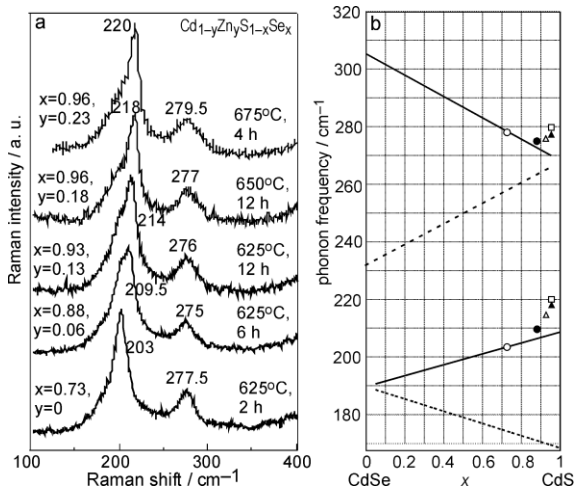

Fig.5 Raman spectra of Se-rich $Cd_{1-y}Zn_yS_{1-x}Se_x$ nanocrystals formed in zinc-containing borosilicate glass doped with Cd, S, and Se, under thermal treatment (a) and compositional dependence of LO (solid lines) and TO (dashed lines) phonon frequencies in $CdS_{1-x}Se_x$ along with the experimental data for the $Cd_{1-y}Zn_yS_{1-x}Se_x$ nanocrystals (b). The spectra were measured using excitation with $\lambda_{exc} = 488.0$ nm.

The increase of zinc amount in the nanocrystals is not linear with the heat treatment duration τ (**Fig. 6**). At $T_a = 625$ °C the limiting Zn concentration $y = 0.19$ is reached at $\tau \approx 8$ h. At higher temperatures the trend is similar, however, higher limiting Zn content values can be reached.

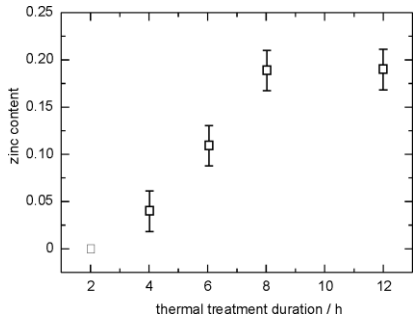

Fig.6 Dependence of Zn content in Se-rich $Cd_{1-y}Zn_yS_{1-x}Se_x$ nanocrystals on the heat treatment duration ($T_a = 625$ °C).

Formation of II–VI nanocrystals in silicate glasses is generally known to comprise three stages – nucleation, diffusion-limited growth and coalescence (competitive growth, or Ostwald ripening) [2–4]. The mechanisms of nucleation and growth for $Cd_{1-y}Zn_yS$ and $CdS_{1-x}Se_x$ nanocrystals in glass matrices are stated to be quite different. Namely, in $Cd_{1-y}Zn_yS$ a stage of homogeneous nucleation is followed by a rapid transition to ripening while $CdS_{1-x}Se_x$ nanocrystals undergo nucleation and growth simultaneously with a gradual transition into the ripening stage [5]. One can expect the growth pattern for quaternary $Cd_{1-y}Zn_yS_{1-x}Se_x$ nanocrystals to be somewhat intermediate, possessing features of both types. In our opinion, fruitful discussion on the competing mechanisms of $Cd_{1-y}Zn_yS_{1-x}Se_x$ nanocrystals growth requires further studies with an extended set of techniques as well as for a variety of samples with a wider range of x and y.

Substitution of Cd by Zn due to thermal diffusion was also reported for CdSe/ZnSe quantum structures grown by molecular-beam epitaxy [27] as well as in CdSe/ZnSe [28] and CdSe/ZnS [29] core/shell nanostructures where Zn atoms from the shell partly replace Cd in the core. An important issue for the discussion of our results is whether within a glass-embedded nanocrystal the distribution of zinc is homogeneous or does it concentrate mostly at the surface. Such effect is not untypical for diffusion of ions from the matrix or substrate into nanocrystals. For example, interdiffusion-related inhomogeneous distribution of atoms in $Si_{1-x}Ge_x$ nanoislands grown by molecular beam epitaxy on Si substrate was reported [30]. Therefore, following Ref. 9, we tried to estimate the duration of cation mixing within a particle at the growth temperature. We did not manage to find the explicit value for zinc diffusion coefficient D in CdS or CdSe, hence we tried to make some estimations using the known expressions for cation self-diffusion in ZnS $D = 4.5\times10^{-3} \exp[-(0.69\ \text{eV}/kT)]\ \text{cm}^2\text{s}^{-1}$ (below 850 °C) [31]. The estimated D for our data ranged from $1.2\times10^{-8}\ \text{cm}^2\text{s}^{-1}$ (625 °C) to $4.8\times10^{-8}\ \text{cm}^2\text{s}^{-1}$ (700 °C). Hence, in assumption of the diffusion process uniformity over the crystallite volume, for the growth duration τ and temperature T_a employed, the diffusion length $L=(D\tau)^{1/2}$ ranged from 1.2×10^{-4} cm (625 °C, 2 h) to 7.6×10^{-4} cm (700 °C, 12 h). As the average nanocrystal diameter ranged from 4×10^{-7} cm (the lowest T_a and the shortest τ) to 9×10^{-7} cm (the most intense heat treatment, 700 °C, 12 h), the duration of Zn cation diffusion through a nanocrystal is less than 1 min. Hence, the duration for the complete mixing of cations in the nanocrystals is much shorter than the heat treatment duration. Therefore, homogeneous distribution of zinc within a nanocrystal can be assumed. However, specific features of the nanocrystal/matrix interface can generally favour near-interface location of one sort of cations. This issue requires more detailed studies, especially by X-ray absorption spectroscopy. It is also the question of further studies whether the limit of zinc content in the nanocrystals is determined only by the glass matrix composition and ratio of Cd and Zn concentrations in the initial mixture, or whether it is restricted by any other effect.

4 Conclusions

The performed Raman scattering studies and SEM imaging data combined with EDX analysis have shown that diffusion of zinc from borosilicate glass matrix to $CdS_{1-x}Se_x$ nanocrystals being formed in the course of diffusion-limited growth at 625–700 °C results in the formation of mixed $Cd_{1-y}Zn_yS_{1-x}Se_x$ nanocrystals with zinc content up to 30 %. The latter can be efficiently evaluated from the LO phonon frequencies in the Raman spectra. An increase of Zn content in the nanocrystals with the thermal treatment temperature and duration is observed. A uniform distribution of zinc over the nanocrystal volume is assumed based on the diffusion coefficient data. More detailed studies are required to find out whether the growth mechanism for these quaternary nanocrystals is predominantly homogeneous or heteogeneous.

References

[1] N.F. Borrelli, D. Hall, H. Holland, D. Smith: Journal of Applied Physics, Vol. 61, 1987, No. 12, p. 5399-5409
[2] L.-C. Liu, S.H. Risbud: Journal of Applied Physics, Vol. 68, 1990, No. 1, p. 28-32
[3] A. Ekimov: Journal of Luminescence, Vol. 70, 1996, No. 1–6, p. 1-20
[4] U. Woggon: *Optical properties of semiconductor quantum dots*. first ed., Springer, Berlin, 1997
[5] M. H. Yükselici: Journal of Physics: Condensed Matter, Vol. 13, 2001, No. 27, p. 6123-6131
[6] Yu.M. Azhniuk et al.: Journal of Crystal Growth, Vol. 312, 2010, No. 10, p. 1709-1716

[7] H. Yükselici, P.D. Persans, T.M. Hayes: Physical Review B, Vol. 52, 1995, No 16, p. 11763-11772
[8] M. Rajalakshmi, T. Sakuntala, A.K. Arora: Journal of Physics: Condensed Matter, Vol. 9, 1997, No. 45, p. 9745-9757
[9] P. D. Persans, L. B. Lurio, J. Pant, G. D. Lian, T. M. Hayes: Physical Review B, Vol. 63, 2001, No. 11, p. 115320-1-115320-8
[10] Yu.M. Azhniuk, A.V. Gomonnai, Yu.I. Hutych, V.V. Lopushansky, I.I. Turok, D.R.T. Zahn: Journal of Physics: Conference Series, Vol. 92, 2007, No. 1, p. 012044-1012044-4
[11] Yu.M. Azhniuk et al.: Physica Status Solidi A, Vol. 201, 2004, No. 7, p. 1578-1587
[12] Yu.M. Azhniuk, A.G. Milekhin, A.V. Gomonnai, Yu.I. Hutych, V.V. Lopushansky, D.R.T. Zahn: Physica Status Solidi C, Vol. 6, 2009, No. 9, p. 2068-2071
[13] S. V. Gaponenko: *Optical Properties of Semiconductor Nanocrystals*. first ed., Cambridge, Cambridge University Press, 1998
[14] A. Tu, P.D. Persans: Applied Physics Letters, Vol. 58, 1991, no. 14, p. 1506–1508
[15] A. Mlayah, A.M. Brugman, R. Carles, J.B. Renucci, M.Ya. Valakh, A.V. Pogorelov: Solid State Communications, Vol. 90, 1994, No. 9, p. 567-570
[16] A. Roy, A. K. Sood: Physical Review B, Vol. 53, 1996, No. 18, p. 12127-12132
[17] A. Ingale, K. C. Rustagi: Physical Review B, Vol. 58, 1998, No. 11, p. 7197-7204
[18] O. Brafman: Solid State Communications, Vol. 11, 1972, No. 4, p. 447-451
[19] W. Meredith et al.: Journal of Crystal Growth, Vol. 159, 1996, No. 1-4, p. 103-107
[20] L.K. Vodopyanov, N.N. Melnik, Yu.G. Sadof'ev: Semiconductors, Vol. 33, 1999, No. 3, p. 283-286
[21] G. Scamarcio, M. Lugara, D. Manno: Physical Review B, Vol. 45, 1992, No. 23, p. 13792-13795
[22] Yu.M. Azhniuk, V.V. Lopushansky, A.V. Gomonnai, V.O. Yukhymchuk, I.I. Turok, Ya.I. Studenyak: Journal of Physics and Chemistry of Solids, Vol. 69, 2008, No. 1, p. 139-146
[23] W.S.O. Rodden, C.N. Ironside, C.M. Sotomayor Torres: Semiconductor Science and Technology, Vol. 9, 1994, No. 10, p. 1839-1842
[24] B. Tell, T.C. Damen, S.P.S. Porto: Physical Review, Vol. 144, 1966, No. 2, p. 771-774
[25] O. Brafman, S. S. Mitra: Physical Review, Vol. 171, 1968, No. 3, p. 931-934
[26] Yu.M. Azhniuk et al: Journal of Physics: Condensed Matter, vol. 16, 2004, No. 49, p. 9069-9082
[27] T. Passow et al.: Physical Review B, Vol. 64, 2001, No. 19, p. 193311-1-193311-4
[28] H. Lee, P.H. Holloway, H. Yang, L. Hardison, V.D. Kleiman: Journal of Chemical Physics, Vol. 125, 2006, No. 16, p. 164711-1-164711-8
[29] V.M Dzhagan, M.Ya. Valakh, A.E. Raevskaya, A.L. Stroyuk, S.Ya. Kuchmiy, D.R.T. Zahn: Nanotechnology, Vol. 18, 2007, No. 28, p. 285701-1-285701-7
[30] M.Ya. Valakh et al.: Nanotechnology, vol. 16, 2005, No. 9, p, 1464-1468
[31] K. Lott, T. Nirk, O. Volobujeva: Crystal Engineering, Vol. 5, 2002, No. 3-4, p. 147-153

Acknowledgements

The research was in part performed in the framework of Slovak-Ukrainian Research and Development Cooperation project No. SK-UA-0024-09. The first author is grateful to Deutsche Forschungsgemeinschaft for the support of his research in Chemnitz University of Technology.